Catalysis Letters 34 (1995) 379–388

Characterization of AlPO systems, precursors of the novel basic catalyst family AlPON

J.J. Benítez, M.A. Centeno, J.A. Odriozola

Departamento de Química Inorgánica e Instituto de Ciencia de Materiales de Sevilla, Centro Mixto Universidad de Sevilla-CSIC, PO Box 874, E-41080 Sevilla, Spain

R. Conanec, R. Marchand and Y. Laurent

Laboratoire de Chimie des Matériaux, URA 1496 CNRS, "Verres et Céramiques", Université de Rennes I, F-35042 Rennes Cedex, France

Received 6 February 1995; accepted 1 June 1995

XPS and DRIFTS (diffuse reflectance infrared spectroscopy) spectra of AlPO systems, formally $AlPO_4-Al_2O_3$, obtained by the sol–gel method have been studied in order to understand their geometric and electronic structure. Both DRIFTS and XPS demonstrate that the acid–base character of these samples depends on a structural modification. For low phosphorus content an amorphous spinel-like solid is proposed. This geometric arrangement alters the electronic density of oxide ions and phosphorus cations and hence their Lewis acid–base properties with respect to the amorphous solid having aluminium and phosphorus only in tetrahedral arrangement.

Keywords: AlPO; aluminum phosphate; DRIFTS; AlPON precursors

1. Introduction

Amorphous aluminophosphates have been shown to be very effective catalysts in a wide variety of processes including dehydrogenation [1], cracking [2] and isomerization [3] reactions. Also as supports of oxidic systems [4–6] or metals [7]. Crystalline $AlPO_4$ is isostructural with silica. The basic building units are AlO_4 and PO_4 tetrahedra. Also, in analogy with silica, amorphous materials with surface areas up to $500\,m^2\,g^{-1}$ have been prepared [8]. Under these conditions the $AlPO_4$ catalysts show acidic properties that can be affected by the modification of the $AlPO_4-Al_2O_3$ ratio, that is the P/Al ratio [2].

Recently, it has been shown that despite the initial acidic character of the starting material, by nitridation of amorphous $AlPO_4$ a new solid with enhanced basic properties (AlPON) can be obtained [9,10]. In this report we study the starting material

by XPS and DRIFTS in order to understand the electronic and geometric changes induced by modifying the P/Al ratio in order to understand the parameters that may affect the nitridation process.

2. Experimental

The sol–gel method developed by Kearby [11] is used to prepare high surface area amorphous oxide precursors ($AlPO_4$). At low temperature, 0°C at most, 3 moles of propylene oxide per mole of aluminium are slowly added to a solution of $AlCl_3 \cdot 6H_2O$ and H_3PO_4 in adequate amounts for obtaining the desired P/Al ratios. At the end of the propylene oxide addition, the pH of the solution increased to a value close to 3. After standing overnight at room temperature, the gel obtained is carefully washed with isopropanol, dried and calcined at 650°C.

Two series (A and B) of amorphous AlPO with variable P/Al ratio have been prepared, table 1. The XPS spectra corresponding to the A and the B series were respectively obtained from a Vacuum Generator 210 and a Physical Electronics 5600 ESCA facility. Both are equipped with a hemispherical analyzer and were respectively operated at 20 and 17.9 eV constant path energy. Mg_K radiation was used in both cases at 240 W for the A series and 400 W for the B series. Peak positions are adjusted to the C_{1s} binding energy at 284.6 eV and 15–20 scans with 0.1 eV steps were accumulated for every region. C_{1s}, Al_{2s}, Al_{2p}, P_{2s}, P_{2p}, O_{1s} and O_{KVV} regions were studied for every sample and the quantitative analysis was done from the atomic sensitivity factors reported in the literature [12].

Prior to the XPS analysis, the A series was outgassed at 100, 250 and 400°C in a preparation chamber with a base pressure of 5×10^{-8} mbar. The temperature was ramped at 10°C/min and kept at the final temperature for 45–60 min. Within this time range the evolution of the pressure in the preparation chamber indicates that the elimination of desorbing species at every temperature is complete. Samples are then cooled and transferred to the analysis chamber with a base pressure of 5×10^{-11} mbar. Specimens corresponding to the B series were calcined at 500°C in a 10°C/min ramp before their introduction in the preparation chamber. After this, they were outgassed overnight at room temperature in the preparation chamber but no further treatment was performed.

Table 1
Atomic composition and specific surface areas of the prepared catalysts

Catalyst	P/Al	Formula	S_{BET} ($m^2\ g^{-1}$)
A16, B27	0.15	$AlP_{0.15}O_{1.875}$	420
A12, B8	0.30	$AlP_{0.30}O_{2.25}$	335
A7	0.60	$AlP_{0.60}O_{3.00}$	490
B4	1.00	$AlPO_4$	395
A1	1.00	$AlPO_4$	300

DRIFTS spectra were collected from a controlled environment cell (Spectra-Tech 0030-101) equipped with ZnSe windows. The cell is mounted in a Nicolet 510P FT-IR spectrometer with a DTGS detector operated at 4 cm^{-1} resolution. A detailed description of this DRIFTS cell has already been given [13]. Samples are heated in situ under a 50 ml/min N_2 flow at 5°C/min for the A series and 10°C/min for the B series. 200 scans are accumulated in each run and no further manipulation but the Kubelka–Munk transformation is performed over the raw spectra.

3. Results

3.1. X-RAY PHOTOELECTRON SPECTROSCOPY

In both series, Al_{2s}, Al_{2p}, P_{2s}, P_{2p} and O_{1s} XPS spectra are characterized as single peaks; no additional structure is observed. The position and shape of these peaks is also independent of the calcination temperature and procedure. Table 2 summarizes the observed binding energy and FWHM (full width at half maximum) values along the complete series. As a reference, the observed values for the A1 and B4 samples, both with P/Al = 1, are in excellent agreement with the data reported by Rebenstorf et al. [4]. From the data in table 2 can be observed a systematic decrease in the binding energy of the different levels as the P/Al ratio is reduced. Fig. 1 shows a plot of the binding energy for Al_{2p}, O_{1s} and P_{2p} levels and the percentage of phosphorus obtained from XPS. The slope of the linear fit is also indicated in the figure. The modification of the slopes with the nature of the level sampled let us discard the relationship found to be due to charge effect. It is also interesting to notice the existence of line broadening in both series for the O_{1s} peak on decreas-

Table 2
Binding energies (eV) and full width at half maximum, in parentheses, for the various catalysts

	P/Al	Al_{2s}	Al_{2p}	P_{2s}	P_{2p}	O_{1s}
A1	1.0	119.8	75.0	191.8	134.4	532.4
		(3.2)	(2.8)	(3.6)	(2.9)	(2.9)
A7	0.6	119.5	74.6	191.5	134.1	532.0
		(3.1)	(2.7)	(3.6)	(2.8)	(2.9)
A12	0.3	119.4	74.6	191.5	134.2	531.8
		(3.2)	(2.7)	(3.6)	(2.9)	(3.3)
A16	0.15	119.0	74.2	191.3	133.9	531.5
		(3.1)	(2.7)	(3.5)	(2.9)	(3.4)
B4	1.0	119.8	75.0	191.7	134.3	532.2
		(2.6)	(2.0)	(3.2)	(2.3)	(2.4)
B8	0.3	119.2	74.4	191.3	133.9	531.7
		(2.7)	(2.2)	(3.2)	(2.4)	(2.7)
B27	0.15	118.9	74.1	191.0	133.8	531.4
		(2.7)	(2.3)	(3.5)	(2.5)	(3.0)

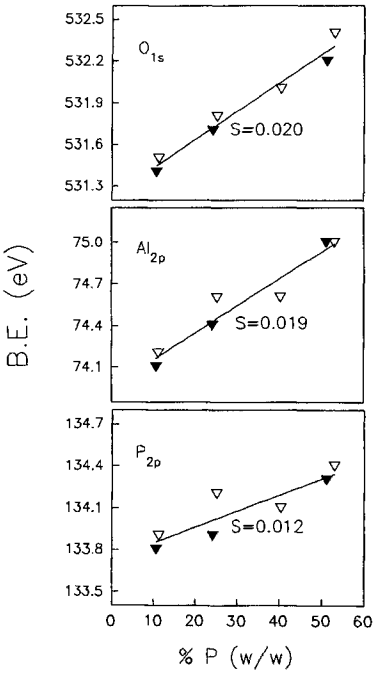

Fig. 1. Evolution of the binding energy of the different levels sampled with the phosphorus content of the catalysts.

ing the P/Al ratio. No such broadening is observed for any other level. The broadening in the O_{1s} peak can be associated with the generation of several types of oxide species at the catalyst surface.

Table 3 shows the atomic composition of the samples as a function of the calcination temperature. Values have been calculated from the XPS peak areas and the reported sensitivity factors [12]. For Al and P the results derived from the 2s and 2p peaks have been averaged. Apart from some minor changes in the atomic percentages, no modification in the P/Al ratio with the calcination temperature is observed. Those minor composition changes are likely due to residual water desorption and to the decomposition of oxygen-containing compounds such as hydroxides and carbonates.

The X-ray excited O_{KVV} spectra for the A series after calcination at 400°C are shown in fig. 2 . Spectra are dominated by two main peaks around 747 and 767 eV respectively corresponding to the $KL_{23}L_{23}$ and the KL_1L_{23} oxygen transitions. A relationship between the separation of these lines (δE) and the ionic character of the oxygen bond has been stated by Wagner et al. [14]. In their study over a wide series of oxides they demonstrated that an increase in the ionic contribution to the oxygen bond is characterized by a decrease in the separation between the oxygen $KL_{23}L_{23}$ and KL_1L_{23} lines. In fig. 2 a plot of the energy difference (δE) between

Table 3
Atomic composition derived from XPS measurements

	T (°C)	Al (%)	P (%)	O (%)	P/Al_{calc}
A1	100	14.2	16.0	69.8	1.13
	250	14.5	16.3	69.2	1.12
	400	14.5	16.4	69.1	1.13
A7	100	18.4	12.2	69.4	0.66
	250	19.1	12.8	68.1	0.67
	400	19.7	13.2	67.1	0.67
A12	100	23.6	7.9	68.5	0.33
	250	24.0	8.1	67.9	0.34
	400	25.5	8.6	65.9	0.34
A16	100	28.4	3.4	68.2	0.12
	250	29.0	3.6	67.4	0.12
	400	29.8	4.1	66.1	0.14
B4	–	15.2	16.5	68.3	1.09
	500	16.5	16.7	66.8	1.01
B8	–	23.4	7.9	68.7	0.34
	500	26.0	7.8	66.2	0.30
B27	–	29.1	3.5	67.4	0.12
	500	30.2	3.6	66.2	0.12

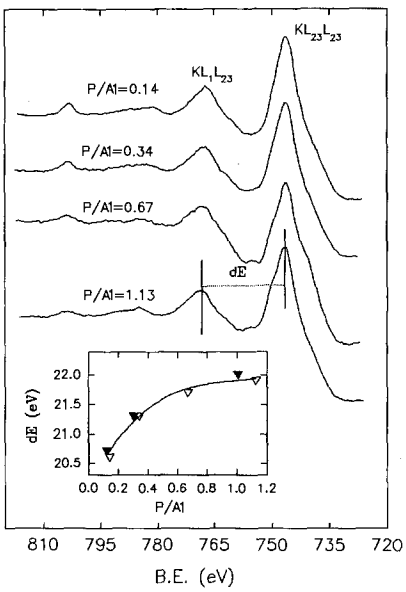

Fig. 2. O_{KVV} spectra for the series A catalysts. The energy separation between the $KL_{23}L_{23}$ and KL_1L_{23} as a function of the XPS measured P/Al ratio is shown in the insert.

these two lines as a function of the P/Al ratio is also shown. As seen in the figure, a decrease in the ionic character of the oxygen bond is expected for high P/Al ratios.

3.2. DIFFUSE REFLECTANCE INFRARED SPECTROSCOPY (DRIFTS)

DRIFTS spectra were obtained at 500°C under N_2 flow for both series. The observed frequencies of the bands are compiled in table 4 and the two main regions of the DRIFTS spectra are shown in fig. 3.

In the 3000–4000 cm^{-1} region two mayor (O–H) stretching bands at 3673 and 3786 cm^{-1} are detected in the A1 and B4 catalysts (P/Al = 1). They are respectively assigned to hydroxyl groups bonded to P and to Al in a tetrahedral environment [15]. Besides this, a shoulder of the high frequency band is also observed at ca. 3770 cm^{-1}; this feature has been previously reported [4] and ascribed to aluminium cations in higher coordination. The frequencies of the (O–H) stretching bands are not modified by the outgassing temperature or the P/Al ratio, table 4. However, when the temperature is increased, a band around 3720 cm^{-1} appears. It corre-

Table 4
Frequencies observed in the DRIFTS spectra of the prepared catalysts as a function of the outgassing temperature

	T (°C)	P(O–H)	Al(O–H)	(P–O)	(Al–O)	Comb.	O–P–O
A1	100	3678	3744	1347	–	773	595
	250	3676	3789	1349	–	775	592
	400	3675	3788	1350	–	769	591
A7	100	3674	–	1297	–	825	–
	250	3675	3789	1318	–	823	603
	400	3673	3787	1314	–	821	596
A12	100	–	–	1256	934	–	–
	250	–	3787	1272	937	–	–
	400	3673	3787	1275	940	–	–
A16	100	–	–	1200	968	–	–
	250	–	–	1215	981	–	–
	400	3673	3781	1217	987	–	–
B4	–	–	–	1295	–	770	578
	500	3673	3788	1353	–	762	590
B8	–	–	–	1252	931	778	–
	500	3671	3786, 3724	1278	932	–	–
B27	–	–	–	1201	967	–	–
	500	3673	3773, 3721	1228	993	–	–

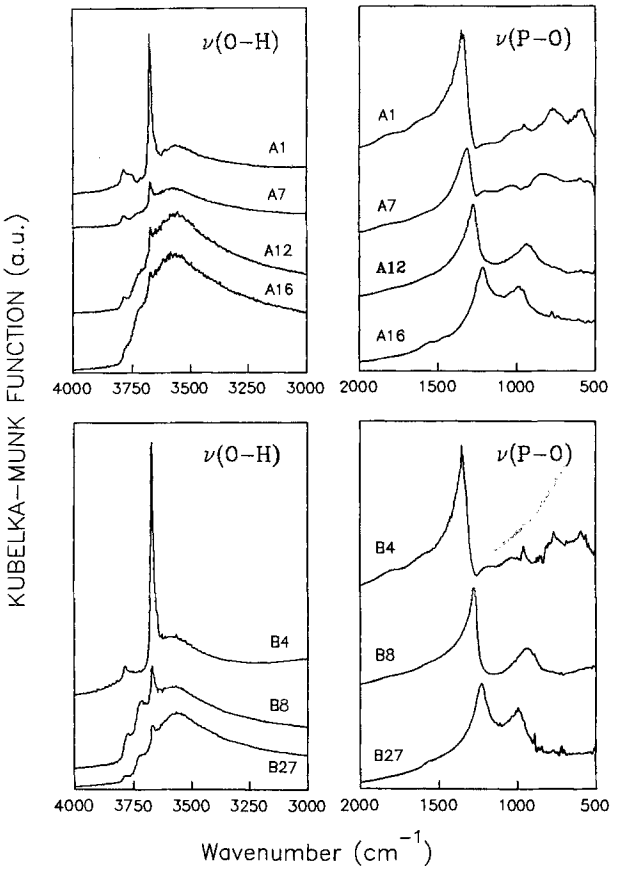

Fig. 3. DRIFTS spectra at 500°C of the studied catalysts under N_2 atmosphere.

sponds to hydroxyl groups bonded to Al in an octahedral disposition [15]. When the P/Al ratio decreases, the band at 3673 cm^{-1} loses intensity and the spectrum is dominated by a broad band at 3550 cm^{-1} assigned to hydrogen bonded hydroxyl groups. The shape of this band and its fine structure is very similar to the one observed for γ-Al_2O_3 [16] which may imply the presence of tetrahedral, pentahedral and octahedral aluminium cations on the catalyst surface [17].

The main band in the 500–2000 cm^{-1} region of the spectra is located in the 1200–1350 cm^{-1} range. This band corresponds to the (P–O) stretching modes [18]. Generic (O–P–O) bending modes are located around 600 cm^{-1} and they are observable in our series when the P/Al ratio is high, mainly in the A1 and B4 samples. In these cases, another band around 775–825 cm^{-1} is produced by the combination of (P–O) and (Al–O) stretching modes.

When the P/Al ratio is low (A12, A18, B8, B27) a band at 900–930 cm^{-1} is developed. The frequency of this new band increases with the Al content and it is assigned to a (Al–O) stretching. The shift towards higher wavenumbers of this

band on decreasing the phosphorus content is consistent with the elimination of phosphorus in the second coordination sphere of aluminium. A similar phenomenon has been previously reported for Sm_2O_3/Al_2O_3 catalysts [19] when the samarium load is reduced.

The most important feature of the DRIFTS spectra is the displacement of the (P–O) stretching band (1200–1350 cm^{-1}) when the amount of phosphorus in the sample is modified, table 4. A high P loading produces a significative upward frequency shift, up to 130 cm^{-1} when the P/Al ratio is reduced from 1 to 0.15. Furthermore, the frequency of the (P–O) stretching band can be directly correlated with the separation between the oxygen Auger lines (δE) in the XPS spectrum, fig. 4. The (P–O) stretching frequency grows in parallel to the line separation. The frequency of the (P–O) stretching mode can be considered as representative of the strength of the (P–O) bond, thus, an increment in the frequency of the band is associated with the reinforcement of the (P–O) bond. The lineal relationship shown in fig. 4 indicates that the increment in the strength of the (P–O) bond is due to the enhancement of its covalent character, which is in turn originated by the increase in the P/Al ratio.

4. Discussion

The structure of amorphous $AlPO_4-Al_2O_3$ catalysts is a subject of major concern. Cheung et al. [20], for instance, examined the structure of aluminophosphates by XRD and ^{27}Al and ^{31}P NMR spectroscopy. They found that the materials were single phase and not a mixture of alumina and aluminophosphate. Similar conclusion has been reached by Babu et al. [1] through, among others, measurements of the activity of the solids in the catalytic conversion of *n*-butanol.

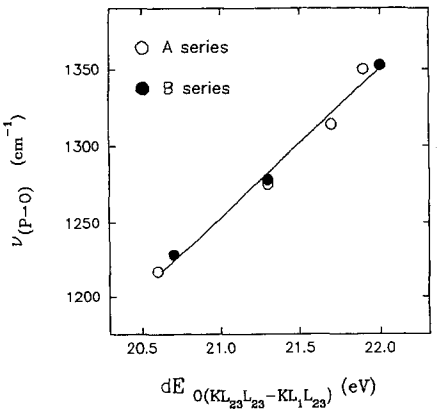

Fig. 4. Correlation between the stretching frequency of the P–O mode and the energy separation of the $KL_{23}L_{23}$ and KL_1L_{23} O_{KVV} Auger lines.

The modification of the binding energies of phosphorus induced by the P/Al ratio, fig. 1, cannot be associated to the alteration of the coordination polyhedra since most of the high resolution NMR spectra on this type of materials suggest that phosphorus is in a tetrahedral environnment [1,20]. So, an electronic density change has to be invoked in such a way that the Lewis acid character of the phosphorus cations is decreased by decreasing the P/Al ratio. This modification also results in an orbital rehybridization that leads to an increase in the covalent character of the oxide ions on the surface, fig. 2. Consequently, the acid–base properties of the surface of the material are affected, as extensively described [21].

The argument based on the modification in the covalent character of the (P–O) bond produced by the alteration of the P/Al ratio can also account for the behaviour of the P and O binding energy observed in fig. 1. The increment in the P_{2p} and O_{1s} binding energy will be produced by the enhancement of the covalent contribution to the (P–O) bond, this is, by the displacement of electronic density from the atomic to the bonding orbitals.

The above described displacement of the electronic density may also affect the acidic character of aluminium cations. However, it has to be taken into account that on modifying the P/Al ratio the stoichiometry of the solid deviates from that of pure $AlPO_4$ up to, formally, $AlP_{0.15}O_{1.875}$. This implies that, in the case of a single phase, the coordination number of aluminium cations has to increase from four up to six. This modification in the coordination number results in a variation of the Madelung potential of the lattice and, in consequence, a shift in the binding energy of aluminium. Thus, the observed sequence for the Al_{2p} level in fig. 1 may be associated both to a change in the electronic structure and to a modification of the Madelung potential of the lattice.

The modification of the environnment of aluminium on modifying the P/Al ratio can be stated from the IR spectra in the hydroxyl stretching region. In fig. 3 features clearly ascribable to hydroxyl coordinated to penta- and octahedral aluminiums, bands around 3725 cm^{-1}, are developed when the P/Al ratio is reduced. Simultaneously, the band associated to Al–O stretching modes shifts towards higher wavenumbers. However, the ones associated to P–O modes move to lower wavenumbers. The upward displacement in the (Al–O) band has to be related to the augment from four to six in the coordination number of aluminium. The shifting in the P–O modes is due to the rehybridization of the orbitals involved in P–O bonds as stated above.

The widening of the O_{1s} signal upon decreasing the P/Al ratio can also be envisaged as a consequence of the presence of several coordination environnments. In this case the first coordination shell can be composed by aluminium, either in a tetrahedral or an octahedral distribution, and phosphorus.

From the reported data it is possible to visualize the structure of the obtained $AlPO_4$–Al_2O_3 catalysts with low phosphorus content as an amorphous phase similar to the spinel-like γ-Al_2O_3 structure in which part of the tetrahedral aluminiums are replaced by phosphorus.

Acknowledgement

This work has been partially financed by the EEC under the COST program (D5/0006/93) and by Comisión Interministerial de Ciencia y Tecnología (MAT94-0434-C03-02).

References

[1] G.P. Babu, P. Ganguli, K. Metcalfe, J.W. Rockliffe and E.G. Smith, J. Mater. Chem. 4 (1994) 331.
[2] J.M. Campelo, A. García, D. Luna, J.M. Marinas, A.A. Romero, J.A. Navío and M.M. Macías, J. Chem. Soc. Faraday Trans. 90 (1994) 2265.
[3] J.M. Campelo, A. García, D. Luna and J.M. Marinas, J. Catal. 102 (1986) 299.
[4] B. Rebenstorf, T. Lindbland and S.L. Andersson, J. Catal. 128 (1991) 293.
[5] S.L. Andersson, Appl. Catal. A 112 (1989) 209.
[6] P.S. Kuo and B.L. Yang, J. Catal. 117 (1989) 301.
[7] J.M. Campelo, A. García, D. Luna and J.M. Marinas, J. Catal. 113 (1988) 172.
[8] J.B. Moffat, Catal. Rev. 18 (1978) 199.
[9] R. Marchand, R. Conanec, Y. Laurent, P. Bastians, P. Grange, L.M. Gandía-Pascual, J. Fernández-Sanz and J.A. Odriozola-Gordon, Patent No. Fr 94 01081.
[10] P. Grange, P. Bastians, R. Conanec, R. Marchand, Y. Laurent, L. Gandía, M. Montes, J. Fernández and J.A. Odriozola, Stud. Surf. Sci. Catal., accepted.
[11] K. Kearby, *Proc. 2nd Int. Congr. on Catalysis*, Paris (Technip, 1961) p. 2567.
[12] D. Briggs and M.P. Seah, eds., *Practical Surface Analysis* (Wiley, Chichester, 1984).
[13] J.J. Benítez, I. Carrizosa and J.A. Odriozola, Appl. Spectry. 47 (1993) 1760.
[14] C.D. Wagner, D.A. Zatko and R.H. Raymond, Anal. Chem. 52 (1980) 1445.
[15] J.B. Peri, Discussions Faraday Soc. 52 (1971) 55.
[16] L.J. Alvarez, J.F. Sanz, M.J. Capitán, M.A. Centeno and J.A. Odriozola, J. Chem. Soc. Faraday Trans. 89 (1993) 3623.
[17] L.J. Alvarez, L.E. León, J. Fernández-Sanz, M.J. Capitán and J.A. Odriozola, Phys. Rev. B 50 (1994) 2561.
[18] V.C. Farmer, ed., *The Infrared Spectra of Minerals* (Mineralogical Society, London, 1974).
[19] M.J. Capitán, P. Malet, M.A. Centeno, A. Muñoz-Paez, I. Carrizosa and J.A. Odriozola, J. Phys. Chem. 97 (1993) 9233.
[20] T.T.P. Cheung, K.W. Willcox, M.P. McDaniel, M.M. Johnson, C. Bronnimann and J. Fryer, J. Catal. 102 (1986) 10.
[21] F.M. Bautista, J.M. Campelo, A. García, D. Luna, J.M. Marinas and A.A. Romero, Appl. Catal. A 104 (1993) 109.